R- 823

Graded Design of EB-PVD Thermal Barrier Coating Systems

U. Schulz, T. Krell, U. Leushake, M. Peters

DLR - German Aerospace Research Establishment, Institute of Materials Research,
D-51147 Cologne, Germany.

Summary

The most durable TBCs (Thermal Barrier Coatings) are yttria partially stabilized zirconia coatings which are applied by EB-PVD (Electron Beam Physical Vapor Deposition) on metallic bond coats. The EB-PVD process offers the advantage of a superior strain and thermoshock tolerant behavior of the coatings due to their columnar microstructure. The interface between ceramic and metal is the weakest link in this system. Spallation occurs in that area which is mainly attributed to oxidation of the bondcoat and to thermomechanical stresses of this two-layered coating.

The concept of graded materials is one approach to lower both stresses and also oxidation of the bondcoat. This concept is presented in detail with special emphasis on chemically graded alumina-zirconia TBCs. Microstructures and phases of alumina, alumina-zirconia, and of graded coatings deposited by EB-PVD are evaluated. Mainly alumina undergoes phase transformation in the mixed and graded layers from the amorphous state to the desired α-Al_2O_3. Finite element modeling was performed to study the influence of coating thickness and composition on heat flux and stress distribution.

1. Introduction

Thermal barrier coatings (TBCs) are increasingly used in gas turbines for aircraft engines and for power generation. They must withstand for a long time heavy thermal cyclic loads under oxidizing conditions. The application range for TBCs in gas turbines includes insulation of the combustion chamber and protection of turbine blades and vanes. Major advantages and key factors that rule the lifetime of TBC systems have been described elsewhere /1, 2/.

Development of gas turbines clearly aims for increased gas turbine inlet temperatures (TIT) passing well beyond 1600°C. Future TBC applications as integral design elements of highly loaded engine parts need a higher temperature capability of the TBC, a better bonding of the ceramic on the metal and also a lower oxidation rate of the bond coat. Thermomechanical stresses caused by this high TIT can only be maintained by usage of uneconomically extensive cooling techniques or by the introduction of electron-beam physical vapor deposited TBCs /3/. The latest generation of TBCs offers significantly extended lifetimes compared to plasma-sprayed TBCs, smooth aerodynamically attractive surfaces and only minor cooling hole closure. The superiority of EB-PVD TBCs is due to their columnar microstructure. Their processing, microstructure, and lifetime in service is often described in literature /1, 4, 5, 6, 7, 8/. But there is still a lack of detailed understanding of failure mechanisms and damage accumulation on a microscopic scale that can be combined with stress modeling, thus enabling a phenomenological based safe life prediction under the wide variety of application conditions.

State-of-the-art TBCs for turbine blades consist of an oxidation protective bond coat (BC) (typically aluminides or MCrAlY, M=Ni, Co), and a thermally insulating yttria partially stabilized zirconia (YPSZ) top layer. This multilayer system is not thermally stable under long time exposure at elevated temperatures. A thermally grown oxide scale (TGO) is formed by oxidation at the BC/zirconia interface. This scale consists mainly of alumina formed by selective oxidation of aluminum from the bond coat but it can vary from this ideal constitution particularly in the early stages of oxidation /9, 10/. The TGO and the interfaces to BC and TBC are the crucial locations of the TBC system that determine in most cases the lifetime. In addition, interdiffusion between the bond coat and substrate leads to microstructural changes in the BC. Another phenomena is the reduction of thermal shock resistance of the zirconia layer due to sintering. Having these phenomena in mind, several potential areas for the application of the Functionally Gradient Materials (FGM) concept for a TBC system can be suggested.

2. Graded Thermal Barrier Coating Systems

Graded materials are characterized by a one or more dimensional continuous or stepwise change of material properties. The change is designed to achieve optimum materials behavior for a given loading situation. FGMs differ from bulk materials and composites by their macro- and microscopic inhomogeneity. To lower residual stresses, coatings can be optimized for the case of fabrication and/or application conditions. Both cases may demand different approaches. The design of graded materials is mainly optimized by numerical or analytical calculations. By applying the FGM concept, changes in the magnitude or location of the critical local stresses can be achieved, although not all stress components are reduced in every case. To improve performance it is often only necessary to modify the stresses which cause failure.

For TBCs a continuously graded layer between bond coat and zirconia would lower the stresses at the interface substantially. Those systems have been described very early for plasma spraying /11/ and for EB-PVD too /12/, but more recently investigations have indicated that they are limited in their potential application. Graded bondcoat-zirconia layers showed improved performance under pure thermal cycling conditions but they suffer from rapid oxidation of BC particles in the zirconia due to their high surface area under oxidizing conditions. This results in a dramatic performance reduction compared to multilayered TBCs /13, 14, 15, 16/. A possible application field for this kind of graded metal-ceramic coating would be limited to non-oxidizing conditions or short time exposure, e.g. reentry. But for turbine engines these graded coatings are not useful.

In 1995 a joint research program on functionally graded materials, funded by the Deutsche Forschungsgemeinschaft (DFG), was started in Germany. Part of this program is the investigation of graded TBCs. It is intended to combine the thermal insulation potential of zirconia with the low oxygen diffusivity of alumina or similar materials. Some results in literature indicate that the introduction of an alumina interlayer between bondcoat and ceramic offers a potential solution to some major problems of TBCs by incorporating a layer with reduced oxygen diffusivity, thereby reducing the TGO growth rate and prolonging cyclic lifetime /17, 18, 19/. These alumina layers has been fabricated by CVD and sputtering techniques. Furthermore, adhesion of EB-PVD PYSZ TBCs is known to be favored on α-alumina compared to adhesion on MCrAlY /10/.

The large mismatch in coefficient of thermal expansion (CTE) between discrete layers within a multicomponent TBC system results in residual stresses that can cause coating failure. Obviously, fully dense alumina layers can not be maintained under thermocyclic loading due to the CTE mismatch. The advantage of a continuously graded coating compared to a single alumina interlayer is the avoidance of a sharp discontinuity in properties and the associated stress concentrations. Starting with alumina on top of the bondcoat a continuous increase of the PYSZ content is envisaged to benefit from the FGM concept. In addition, by controlled oxide/TBC interface formation, better adhesion and reduced thermal stresses may be realized. Among the large variety of alumina polymorphs, α-Al_2O_3 is the most desirable phase because of its low oxygen diffusivity and high thermal stability at the application temperature range. Therefore, one target is to get α-alumina. All ceramic layers within the graded TBC are produced by PVD techniques, preferentially by high rate EB-PVD.
Another possibility to apply the FGM concept to TBCs would be a graded layer between metallic bondcoat and an alumina interlayer. This approach would harden the bond coat outer region and therefore lower the creep rate of MCrAlY. Furthermore, improved adhesion of the alumina is expected but some processing problems will occur too.

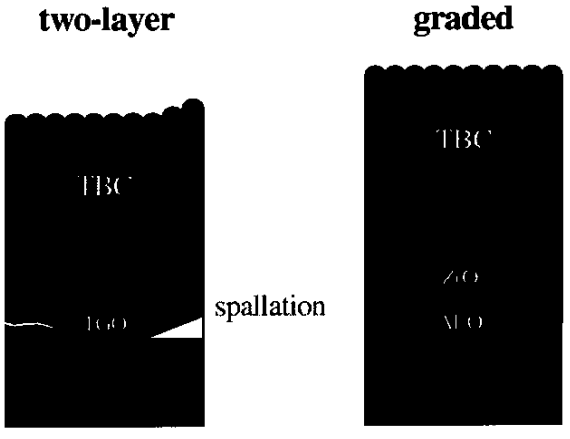

Fig. 1: Comparison of conventional and graded design of TBCs

Fig. 1 shows the state-of-the art two-layer coating compared to the new proposed graded ceramic design. First results of the work carried out on this graded TBC system have been published previously /20, 21, 22/.

2.1 Processing of graded TBCs

In order to combine the advantages of columnar and graded structures several issues must be incorporated. The vaporization during EB-PVD depends on the vapor pressure of each compound which makes it difficult to simultaneously vaporize materials with large differences in vapor pressure (e.g. ZrO_2 and CeO_2). Using a single source coater only certain chemical gradients can be produced, although some types of gradients have been successfully produced, e.g. density graded PYSZ and chemically graded bondcoats /23, 24/. Another attempt is the use of a special mixture of aluminum, alumina, and zirconia as a starting composition in form of pressed tablets on top of YPSZ ingots to get a graded structure /25/. Controlled chemically graded coatings can be fabricated by vaporizing from multiple sources utilizing one or more electron guns.

To develop the graded TBC system described above several problems had to be solved in advance:
- evaporation material must be in a condition that allows continuous evaporation
- influence of evaporation conditions on microstructure of single alumina layers must be evaluated
- dual source evaporation of alumina and zirconia to get mixtures of both species must be established.

Finally, grading from alumina to YPSZ was carried out.

2.2 Experimental procedure

In the present study, a single gun dual source jumping electron beam coater was used (for details see /5/). It consists of chambers for loading, preheating and deposition and facilities for specimens rotation and manipulation. Ingots of 50 mm and 63 mm diameter were fed into the crucibles from bottom during evaporation in order to ensure continuous deposition. By adjusting electron beam parameters different deposition rates can be achieved for each source via independent adjustment of melting pool temperatures. Alumina films were deposited by reactive magnetron sputtering and also by reactive EB-PVD.

X-ray diffraction (XRD) was carried out with Cu K_α radiation. If not noticed explicit otherwise patterns are given corrected for background and $K_{\alpha 2}$. Concentration was measured quantitatively by energy dispersive X-ray spectroscopy on polished cross sections.

3. Results and discussion

3.1. Alumina ingots

Semi-industrial or industrial size coaters use a continuous feeding system for ceramic rod source materials (ingots). They must exhibit a high thermal shock resistance to withstand the high thermal gradients associated with EB-PVD processing. Therefore, ingots generally have a relative density of about 60%. The current processing method for YPSZ ingots involves powder and material specific sintering and calcination and cannot easily be transferred to other powders or materials. An alternative method was developed that involves the use of bimodal powder mixtures and a sinterless powder metallurgical processing /21, 22, 26/. This processing route can be applied to a large variety of different powders and materials for ceramic rod fabrication, achieving suitable vaporization behavior and high thermal shock resistance at low cost.

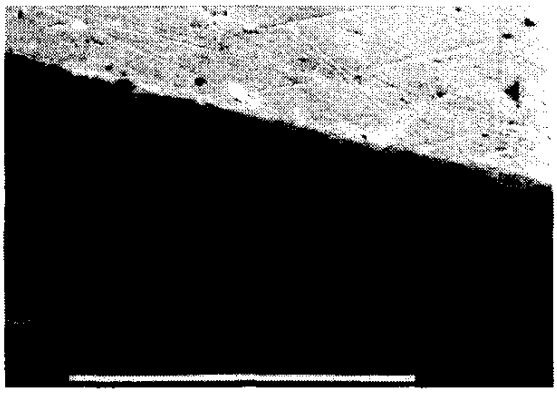

1 mm

Fig. 2: Cross section of a thick alumina coating obtained by EB-PVD at low pressure

3.2. Alumina coatings

Phase content and morphology of alumina coatings, produced by PVD methods, were investigated as a function of process parameters. Chamber pressure during alumina evaporation was varied by an optional additional oxygen gas flow and by adjustment of the pumping rate in order to achieve in some experiments reactive conditions.

In the case of lower chamber pressures, extremely high ceramic deposition rates up to 60 µm/min occurred. In Fig. 2 an example is given for a coating deposited under such conditions. It can be concluded that higher deposition rates and the associated lower chamber pressures result in relatively dense, less columnar microstructures, probably as a result of changed adatom mobility /22/.

On the other hand, a 5 to 8 µm thin alumina layer deposited by EB-PVD under reactive conditions exhibits a columnar microstructure. After annealing a tendency to sintering was observed /20/.

Thin alumina layers produced by reactive magnetron sputtering showed a rough surface which reproduces the surface of the underlying metal as it is characteristic for PVD. In Fig. 3 an example is given where the bond coat morphology is still visible because peening was omitted.

Obviously, the morphology of alumina films produced by PVD strongly depends on deposition parameters and for sputtering on the substrate surface too. Deposition rate, chamber pressure and atmosphere, film thickness, and substrate temperature are the most important parameters that rule the morphology of alumina.

In the temperature range of deposition alumina undergoes phase transformations, so that not only microstructure of the coatings but also phase formation depends on the substrate temperature. It was intended to get the most stable alpha phase of alumina.

Alumina deposition was carried out in the temperature range between 750 and 1150°C. In Fig. 4 the influence

10 µm

Fig. 3: Surface of sputtered alumina layer on top of NiCoCrAlY bondcoat

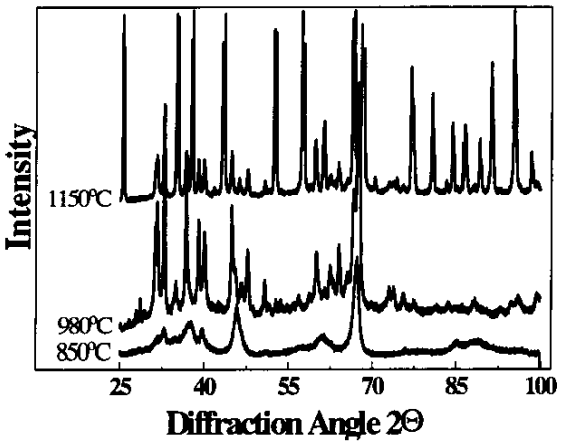

Fig. 4: XRD of EB-PVD alumina films for various deposition temperatures (not corrected)

of deposition temperature on phase formation of alumina is shown.

XRD peaks were broadened for alumina films deposited at low temperatures. This can be attributed to the presence of areas within the coating that were not fully crystallized. Coatings deposited at the highest temperature showed the presence of only the stable α-Al_2O_3 phase. Additionally it was found that chamber pressure and deposition rate had only little influence on phase formation of alumina which is contrary to results found for the morphology.

Phase transformation was also studied after annealing in the temperature range between 1000°C and 1200°C for 1 to 9 hrs. Annealing at 1000°C had little effect on any of the coatings; only a sharpening of diffraction peaks was observed. For all coatings, transformation to α-Al_2O_3 started upon annealing at 1100°C. Short term (1 h) annealing at 1100°C resulted in partial transformation to α-Al_2O_3. The higher the deposition temperature was, the lower was the tendency for phase transformation. This can be explained by the fact that the driving force for transformation (i.e. difference between coating and annealing temperature) is lower. After annealing at 1200°C for 9hrs all coatings consisted mainly of α-Al_2O_3 with only small amounts of other phases /21, 22/.

Alumina layers deposited by reactive magnetron sputtering were amorphous but they showed a rapid phase transformation behavior. Observations are in good agreement with literature data on alumina layers obtained by sputtering /27, 28/ and by reactive aluminium evaporation /29/.

As a consequence, alpha alumina coatings can be achieved either by in-situ deposition at elevated temperatures or by post coating anncaling. Since the phase transformation driving force is proportional to the temperature difference between the coating temperature and the annealing temperature, coatings deposited at lower temperature show faster phase transformation.

3.3. Mixed alumina-zirconia layers

Due to the continuous change of composition and properties within a graded alumina - PYSZ coating a direct analyses of phases is difficult. Therefore, mixtures of alumina and PYSZ were investigated. They represent individual layers of the graded ceramic.

Co-evaporation of alumina and PYSZ was carried out using the jumping-beam technique. First, vaporization parameters such as scanning pattern, e-beam focus, dwell time and vapor cloud geometry were determined for each material separately. The several mixtures of alumina/PYSZ with various amounts of the oxides were produced by dual source evaporation.

In Fig. 5 chemical composition is plotted as a function of sample position above the ingots. Experiments clearly show that dual source evaporation of two ceramics with widely differing vapor pressures and melting points is possible using the jumping-beam technique. A mixing of both ceramic vapor clouds takes place and both species condense on the substrates thereby forming mixed layers. While the portion of Al_2O_3 decreases more rapidly with decreasing distance to the ZrO_2-ingot, the portion of ZrO_2 rises slower and shows a flatter gradient. The zirconia content is predominant in all coatings. The reason for that is the difference of vapor pressures and evaporation behavior between ZrO_2 and Al_2O_3 that leads to a different geometry of the vapor clouds. Furthermore it can be assumed that the re-evaporation rate of alumina is higher than that of zirconia because of its lower melting and boiling point.

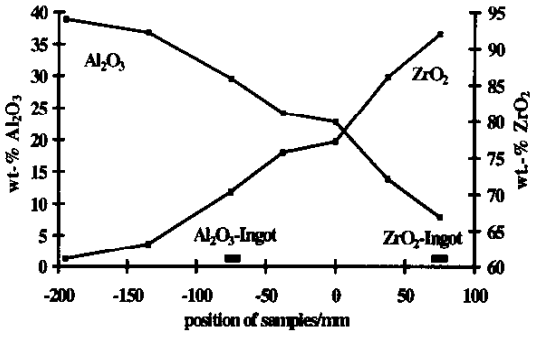

Fig. 5: Composition of mixed alumina-PYSZ layers as a function of position in the chamber

The morphology of these coatings is exemplified in Fig. 6. All coatings have a columnar microstructure, but contrary to pure PYSZ TBCs the alumina-zirconia coatings show a much more closely packed structure.

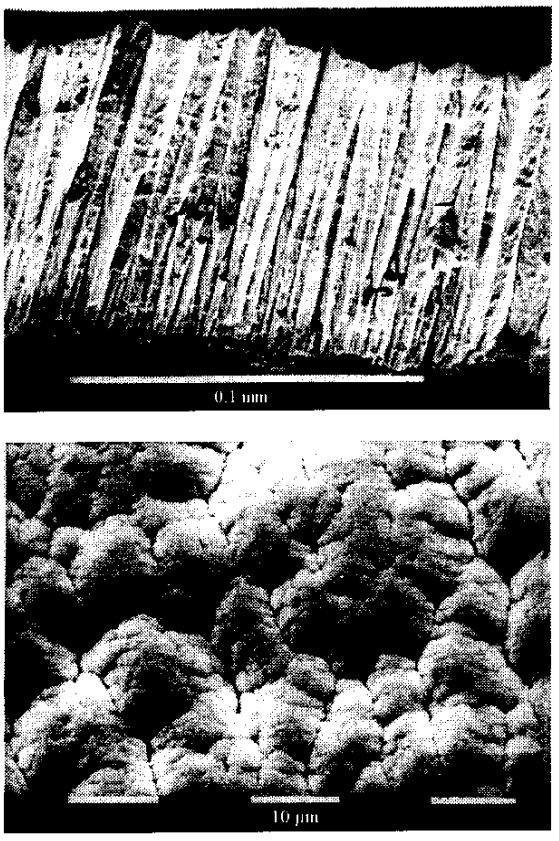

Fig. 6: SEM of mixed alumina-PYSZ layers, fractograph (above) and surface (below)

Moreover, surfaces of the columns are no flat faces with characteristic shapes as it was found for yttria and ceria stabilized zirconias /30/, but they are round shaped with cauliflower type appearance. Furthermore they posses less opened inter-columnar porosity. Even small amounts of alumina can cause these microstructural changes. Since microstructure was nearly the same for all mixtures, one can conclude that not the amount of alumina but the presence itself is sufficient for the change in morphology.

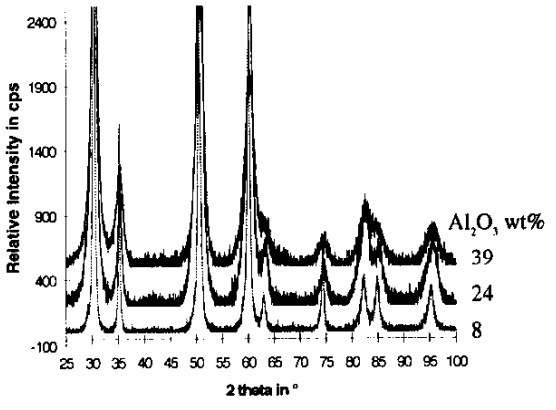

Fig. 7: XRD of EB-PVD mixed coatings from alumina and PYSZ

Results of XRD are shown in Fig. 7.
Phase analyses only reveals strongly broadened PYSZ-peaks which are getting sharper with increasing content of zirconia. No alumina peaks were found in the as coated condition. This suggests that alumina only exists as an amorphous phase, but it is not clear where this phase is located beside the zirconia crystals. Additional investigations by transmission electron microscopy are under way in order to clarify this question.

Because of the broadened peaks zirconia must be very fine grained which is contrary to pure PYSZ TBCs where each column is nearly single crystalline. A first calculation of the grain size based on zirconia peak half-width gave evidence for 5-15 µm grains, depending on the alumina content. Thermal conductivity and other properties of this fine-grained two-phase structure may significantly differ from values that were calculated using simple rules of mixture. Since lattice parameters of PYSZ are only slightly changed by the addition of alumina one can conclude that only small amounts of alumina were incorporated into the tetragonal lattice of the t' phase of PYSZ.

3.4. Graded alumina-PYSZ thermal barrier coatings

By continuously changing the evaporation rates of alumina and zirconia a change in composition over the coating thickness was achieved. Due to the different deposition conditions which are necessary to maintain suitable evaporation of alumina, zirconia and various mixtures thereof, an increase of the substrate temperature occurs with increasing zirconia content in the vapor cloud.
Initially a pure and thin alumina layer was put on top of a NiCoCrAlY bondcoat, followed by compositional graded mixed alumina - PYSZ layers. At the top side pure PYSZ was deposited. A cross-section of such a graded coating is shown in Fig. 8. The backscattered electron imaging (right part of picture) indicates a steep gradient in chemical composition between alumina and zirconia. In contrast, change of microstructure from bottom (alumina) to top (zirconia) appears not continuous.

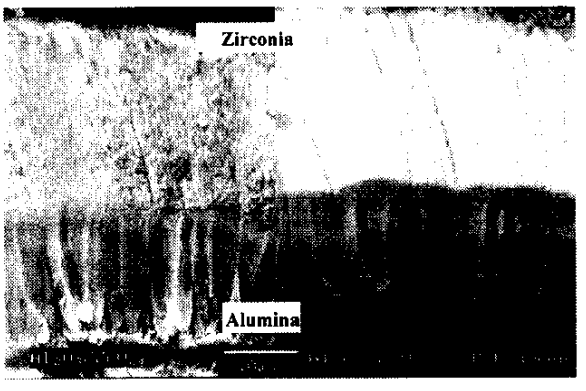

Fig. 8: Cross section of a graded alumina-PYSZ TBC

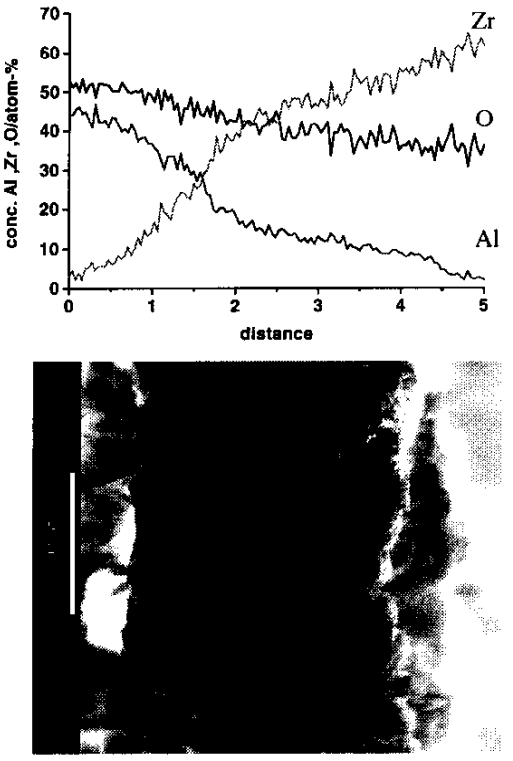

Fig. 9: Graded alumina-PYSZ coating, composition (above) and fractograph (below)

Fig. 9 evidences a continuous chemical gradient. For better visibility the graded layer is shown as a fractured cross section.
Although there is still a step in the gray-scale of the SEM picture the concentration profile shows only a slightly steeper change of concentration in this area.

Experiments have revealed that two-source evaporation can produce a distinct graded layer although only one electron-beam gun has been used. Application of jumping beam technology on ceramics requires a fast beam deflection system with capability of beam scanning frequencies up to 1 kHz. It was found that adjusting the beam pattern and beam focus to the different ceramics was the key point for a reproducible evaporation behavior and also to omit spitting mainly from the alumina ingot. This task is complicated because zirconia needs approximately two to three times more energy for evaporation but beam power cannot be changed quickly during the jumping procedure.

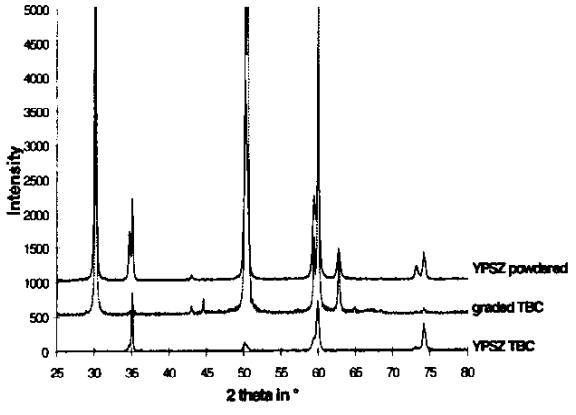

Fig. 10: XRD of different EB-PVD TBCs

To illustrate the problems of microstructure investigation of graded layers XRD patterns of a graded, a standard PYSZ TBC, and a powdered PYSZ TBC are compared in Fig. 10.
The absence of any alumina peaks in the graded layer must be noticed which is similar to observations on mixtures. The thin PYSZ layer on top of the graded zone additionally complicates the investigation of the FGM because of the low x-ray penetration depth in zirconia. The highly textured growth of both EB-PVD coatings can be seen but some differences in the preferred orientation can be already determined from simple diffraction patterns. While PYSZ TBCs grow primarily with {100} planes parallel to the surface /5, 31/ the graded layers posses mainly strong {220} and {113} peaks. Taking into account the results of mixed layers (Fig. 7) it is obvious that alumina additions to PYSZ lower the tendency to preferred growth of some crystallographic orientations. The fine grain size within graded layers instead of single crystalline columns in case of pure PYSZ may further contribute to the observed texture differences.

In a final step the fully ceramic graded thermal barrier coating system was produced. One important aspect to consider is the change in overall thermal conductivity of the graded layer due to the higher thermal conductivity of alumina compared to zirconia. This also depends on the compositional gradient itself, and it has to be compensated by an additional zirconia layer. Numerical and analytical computations can help to calculate the appropriate thermal fluxes and thicknesses of the individual layers. This topic will be discussed in chapter 4.
A standard PYSZ-TBC of approximately 200 µm thickness was applied on top of the graded layer in order to maintain the desired thermal conductivity of the whole system. The TBC is shown in Fig. 11.

The zirconia layer on top exhibits the desirable columnar microstructure typical for EB-PVD coatings. The graded region, however, is characterized by a coarser microstructure within the columns and a smaller column diameter. Here, spacings between columns seem to be smaller and the FGM looks more compact compared to the opened columnar PYSZ region. The temperature increase during evaporation mentioned above may have further supported occurrence of this morphology. Columns go through from the graded zone to the PYSZ top layer which is necessary for a good bonding. Micro-

structural features are in good agreement with observations on mixed layers described in chapter 3.3.

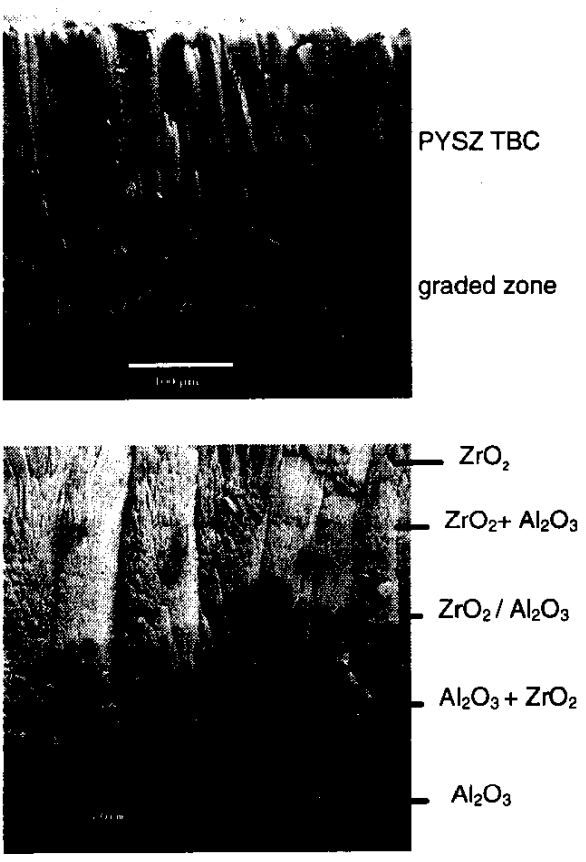

Fig. 11: Morphology of a ceramic graded EB-PVD TBC system

4. Finite Element Modeling for graded TBCs

Finite Element Method (FEM) and analytical calculations provide a useful tool for an understanding of complex thermal and stress fields. The reliability of the calculations depends strongly on the used material properties and boundary conditions. Assumptions like pure linear elastic behavior or certain boundary conditions may have a substantial effect on the results. In most cases the microstructure is modeled on a macroscopic scale, since the real columnar microstructure of EB-PVD or the splashy one of plasma sprayed coatings is to complex for a microscopic model. Calculations are based on knowledge of material properties. For bulk materials, most properties are known or can be measured. For coatings, however, data availability is limited. This may cause some uncertainties about the accuracy of stress calculations and finite element modeling. The properties of composites are often estimated by different rule of mixtures according to their microstructure.
The designing process of FGMs should include the calculation of thermal fields and their stresses and also residual stresses during fabrication. For a complete calculation of the stress state effects like creep, plastic deformation, oxidation, and sintering have to be taken into account. It must contain also stresses after fabrication, in the transient stages, in the temperature field during service and after cooling down to room temperature. All these aspects described above have to taken into account in order to draw the right conclusions from calculations.
In the following one special aspects of the design of graded TBCs will be explained in detail.

The designing process is based on a parametric variation of a chosen grading function, which describes the change in chemical composition along the coating thickness. Widely used is a simple power law function:

$$c(x) = \left(\frac{d}{h}\right)^p = x^p \qquad (1)$$

where c is the concentration, d the distance to the interface or surface, h the coating thickness, x the normalized height and p the profile parameter. By variation of the profile parameter p different chemical profiles are defined and according to the local composition and microstructure the local material properties can be set. A widely used approach is that the grading function also directly describes the variation of material properties.
Variation of the profile parameter p leads to different stress situations and the minimization of the critical stress component responsible for failure can be defined as an optimum. Variation of the grading function also effects the FGMs overall thermal conductivity and therefore the thermal field. In case of a constant coating thickness and of boundary conditions that are given by fixed surface temperatures the heat flux depends on the profile parameter. If the boundary conditions are set different the maximum temperature of the metal may exceed a certain value. These variations complicate the comparison of calculated stress fields and the design process has to be extended to take this effect into account. The variation of coating thickness itself and the corrected thermal boundary conditions affect the stress distribution in the graded system.

Thermal conductivity of alumina is substantially higher than that of zirconia and therefore the thickness of the graded coating has to be increased. The increase can be calculated by defining an effective thermal resistivity R:

$$R^* = \int_0^1 \frac{1}{\lambda(x)} dx \qquad (2)$$

with x the normalized height, $\lambda(x)$ the local thermal conductivity. In combination with different rules of mixtures for the thermal conductivity of composites and the grading function (1) the effective thermal resistivity R^* can be calculated either analytically or numerically.

Fig. 12 shows the effect of the profile parameter p on the effective thermal resistivity. These curves can be used to estimate coating thicknesses of same heat flux. To meet

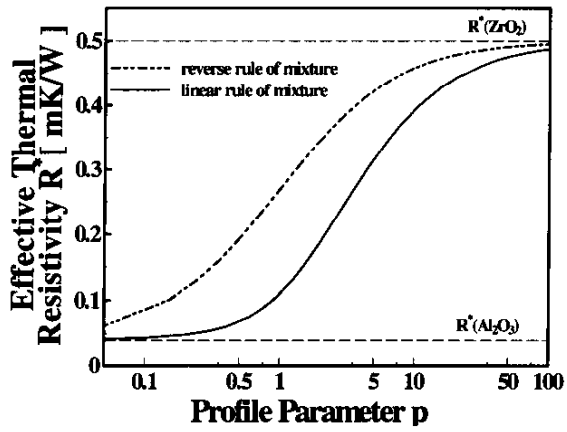

Fig. 12: Effective thermal resistivity for different rules of mixtures and profile parameters

this requirement, thickness has to be increased by a factor of 4.6 in case of a linear graded layer compared to pure PYSZ. Increase of coating thickness is limited to a certain level for aero engines. Therefore application of an additional zirconia layer on top of the graded layer is preferred to get same heat fluxes.

For a loading situation similar to a turbine blade stresses of different coating systems have been calculated (Fig. 13). In a biaxial stress state the radial stresses of an infinite plate have been calculated assuming linear elastic behavior /32. The model involves a 1mm thick superalloy substrate that possesses a NiCoCrAlY bondcoat of 150 µm and the TBC on top. All material properties were assumed to follow the linear rule of mixture and to be not temperature dependend which causes only little

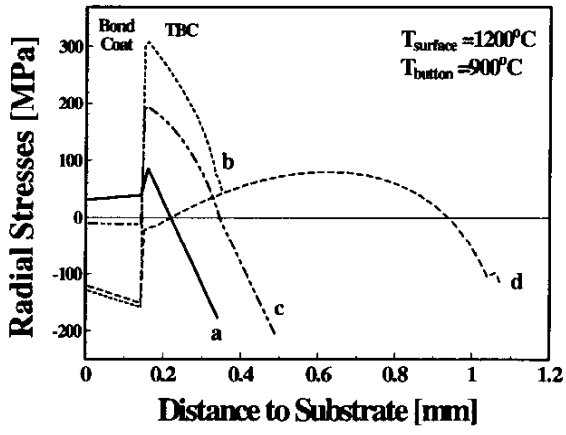

curve	ZrO2 µm	FGM µm	heat flux MW/m²
a	200	0	2
b	0	200	4.2
c	150	200	2
d	0	920	2

Fig. 13: Effect of corrected coating thickness on stress distribution

deviations because of small temperature gradients.
Compared to a non-graded TBC of 200 µm ZrO_2 (curve a) the heat flux of a linear graded coating with the same thickness (curve b) is more than twice as high. In this case the graded layer shows higher interfacial tensile stress, which should decrease performance. Based on (1) and (2) the overall thickness of the graded layer was increased to same heat flux conditions (curve d), resulting in the lowest compressive interface stresses in the ceramic but in a dramatic higher thickness too. Alternatively, a 150 µm thick zirconia layer was applied on top of a 200 µm thick graded layer (curve c), resulting in the same heat flux as the conventional system. Stresses in the bondcoat are much lower than for all other systems, but interfacial stresses are higher compared to a and d. From these examples one can see that the grading profile significantly influences the stress situation. For optimization, knowledge of critical stresses that are responsible for failure is essential. In case of coating thickness of same heat flux the FGM concept offers a potential for improvement of coating performance.

5. Conclusions

The potential of chemically graded thermal barrier coatings to improve lifetime and reliability of turbine blades was evaluated. It has been demonstrated, that graded ceramic coatings can be produced by dual source EB-PVD and jumping beam technology. Various mixtures of alumina-PYSZ as well as pure alumina and graded coatings have been produced and analyzed.

1. Morphology and phases of PVD alumina films depend on deposition parameters, mainly on deposition rate, chamber pressure and atmosphere, film thickness, and substrate temperature. Alpha alumina can be obtained either by high substrate temperatures or by post coat annealing.
2. Morphology of alumina-zirconia mixtures is more compact than that of pure YPSZ TBC but it depends to a less extend on the amount of alumina. Zirconia is very fine grained in an amorphous alumina matrix.
3. By defining an effective thermal resistivity coating thickness can be adapted to constant heat flux conditions With a graded transition zone and with a modified coating thickness a variation of the stress field can be achieved.

Optimization of coating conditions and the design of the graded zone with respect to chemical composition profile, phases, microstructure, morphology, and optimized lifetime remains to be carried out in future research.

ACKNOWLEDGEMENTS

The authors gratefully acknowledge technical support by J. Brien, C, Kröder, H. Mangers and H. Schurmann.. The work was partially funded by the Deutsche Forschungsgemeinschaft.

References

1 Kaysser et al. AGARD this issue

2 M. Peters, K. Fritscher, G. Staniek, W.A. Kaysser, U. Schulz: Design and properties of thermal barrier coatings for advanced turbine engines. Materialwissenschaft und Werkstofftechnik 28(1997) 357-362

3 J.T. DeMasi-Marcin and D.K. Gupta, "Protective Coatings in the Gas Turbine Engine", Surface and Coatings Technology 68/69 (1994)1-9

4 S.M. Meier, D.M. Nissley, K.D. Sheffler, T.A. Cruse: "Thermal barrier coating life prediction model development", ASME J. Eng. Gas Turbine Power 114(1992) 258-263

5 U. Schulz, K. Fritscher, C. Leyens, M. Peters, W.A. Kaysser: Thermocyclic Behavior of Differently Stabilized and Structured EB-PVD Thermal Barrier Coatings. Materialwissenschaft und Werkstofftechnik 28(1997) 370-376

6 Schulz, U.; Fritscher, K.; Rätzer-Scheibe, H.-J.; Peters, M.; Kaysser, W.A.: Thermocyclic Behaviour of Microstructurally Modified EB-PVD Thermal Barrier Coatings. 4th International Symposium on High Temperature Corrosion and Protection of Materials. Les Embiez 20-24.5.1996

7 Sohn, Y.H.; Biederman, R.R.; Sisson Jr, R.D.: Microstructural development in physical vapour-deposited partially stabilized zirconia thermal barrier coatings. Thin Solid Films 250(1994)1-7

8 Maricocchi, A.; Bartz, A.; Wortman, D.J.: PVD TBC experience on GE Aircraft engines. Proc. TBC workshop Cleveland 1995, ed. W.J. Brindley, NASA Conf. Publication 3312 (1995) 79-89

9 Schmücker, M.; Fritscher, K.; Schulz, U.: Haftmechanismen in ausgewählten EB-PVD Wärmedämmschichtsystemen. Fortschrittsberichte der DKG, Werkstoffe, Verfahren, Anwendung 10(1995)4, 379-384

10 Fritscher, K.; Schmücker, M.; Leyens, C.; Schulz, U: TEM Investigation on the Adhesion of EB-PVD Thermal Barrier Coatings. 4th International Symposium on High Temperature Corrosion and Protection of Materials. Les Embiez 20-24.5.1996

11 Goward, G.W.; Grey, D.A.; Krutenat, R.C.: US Patent No. 4 248 940

12 Jamarani, F.; Korotkin, M.; Lang, R.V.; Ouelette, M.F.; Yan, K.L.; Bertram, R.W.; Parameswaram, V.R.: Compositionally graded thermal barrier coatings for high temperature aero gas turbine components. Surface and Coatings Technology 54/55(1992) 58-63

13 Ulion, N.E.; Ruckle, D.L.: Columnar grain ceramic thermal barrier coatings on polished substrates. European Patent EP 0044329B1

14 Alaya, M.; Grathwohl, G.; Musil, J.: A comparison of thermal cycling behaviour of graded and duplex ZrO_2-thermal barrier coatings. Proc. FGM'94, eds. B.Ilschner et al. Lausanne (1994) 405-411

15 Lee, W.Y.; Stinton, D.P.; Berndt, C.C.; Erdogan, F.; Lee, Y-D.; Mutasim, Z.: Concept of functionally graded materials for advanced thermal barrier coating application. J. Am. Ceram. Soc. 97 (1996) 12, 3003-3012

16 Vincenzini, P.: Zirconia thermal barrier coatings for engine applications. Industrial Ceramics 10(1990)3, 113-126

17 Schmitt-Thomas, Kh.G.; Dietl, U.: Surface and coatings technology, 68/69 (1994) 113-115

18 Sun, J.H., Chang, E.; Wu, B.C.; Tsai, C.H.: The properties and performance of (ZrO_2-8wt%Y_2O_3)/(chemically vapour-deposited Al_2O_3)/(Ni-22wt%Cr-10wt%Al-1wt%Y) thermal barrier coatings. Surface and Coatings Technology 58(1993) 93-99

19 Strangman, T.E; Solfest, P.A.: Ceramic thermal barrier coating with alumina interlayer. US Patent 5 015 502 (14.5.1991)

20 T. Krell, U. Schulz, M. Peters, W.A. Kaysser: Influence of various process parameters on morphology and phase content of EB-PVD thermal barrier coatings. Poc. EUROMAT 97, eds. L.A.J.L. Sarton and H.B. Zeedijk, Netherlands Soc. for Materials Science, Vol. 3(1997) 3/29-3/32

21 U. Leushake, U. Schulz , T. Krell, M. Peters, W.A. Kaysser: Al_2O_3 - ZrO_2 Graded Thermal Barrier Coatings by EB-PVD - Concept, Microstructure and Phase Stability. Proc. 4th Int. Symp. on FGM'96.

22 U. Leushake, T. Krell, U. Schulz, M. Peters, W.A. Kaysser: Microstructure and Phase Stability of EB-PVD Alumina and Alumina/Zirconia for Thermal Barrier Coating Application. ICMCTF '97, Surface and Coatings Technology (in press)

23 Fritscher, K.; Schulz, U.: Burner-rig performance of density-graded EB-PVD processed thermal barrier coatings. in "Ceramic Coatings" ed. K.Kokini, New York, ASME MD-Vol.44 (1993) 1-8.

24 Schulz, U.; Fritscher, K.; Peters, M.; Kaysser, W.A.: Processing and behavior of chemically graded EB-PVD MCrAlY bond coats. Proc. FGM 94, eds. B. Ilschner, N. Cherradi, Presses polytechniques et universitaires romandes (1995), Lausanne, 441-446

25 Movchan, B.A.: EB-PVD technology in the gas turbine industry: present and future. JOM 11(1996) 40-45

26 U. Leushake, W. Luxem, C.-J. Kröder, W.-D. Zimmermann: German patent application #A19623587.1, European patent application No. 97108972.7-2111

27 J. A. Thornton, J. Chin: Structure and Heat Treatment Characteristics of Sputter-Deposited Alumina, Ceramic Bulletin, 56 5 (1977) 504-508

28 R. F. Bunshah, R. J. Schramm: Alumina Deposition by Activated Reactive Evaporation, Thin Solid Films, 40 (1977) 211-216

29 A. L. Dragoo, J. J. Diamond: Transitions in Vapor-Deposited Alumina from 300-1200°C, Journal of The American Ceramic Society, 50, 11 (1967) 568-574

30 Schulz, U.; Fritscher, K.; Peters, M.: EB-PVD Y_2O_3 and CeO_2/Y_2O_3 Stabilized Zirconia Thermal Barrier Coatings - Crystal Habit and Phase Composition. Surface and Coatings Technology 82 (1996) 259-269

31 Schulz, U.; Oettel, H.; Bunk, W.: Texture of EB-PVD thermal barrier coatings under variable deposition conditions. Zeitschrift für Metallkunde 87(1996)6, 488-492

32 M. Finot, S. Suresh, Multitherm, MIT